

RESEARCH

Open Access



Effect of drought on photosynthesis, total antioxidant capacity, bioactive component accumulation, and the transcriptome of *Atractylodes lancea*

Aqin Zhang^{1,2†}, Mengxue Liu^{1†}, Wei Gu^{1,3*}, Ziyun Chen¹, Yuchen Gu¹, Lingfeng Pei¹ and Rong Tian¹

Abstract

Background: *Atractylodes lancea* (Thunb.) DC, a medicinal herb belonging to the Asteraceae family, often faces severe drought stress during its growth. Until now, there has been no research on the effect of drought stress on the quality formation of *A. lancea*. Therefore, the present study aimed to study the effects of drought stress on *A. lancea* through physical and chemical analysis, and to reveal the related molecular mechanisms via transcriptome analysis.

Results: The photosynthesis was markedly inhibited under drought stress. There were alterations to photosynthetic parameters (Pn, Gs, Ci) and chlorophyll fluorescence (Fv/Fm, NPQ), and the chlorophyll content decreased. Twenty genes encoding important regulatory enzymes in light and dark reactions, including the Rubisco gene of the Calvin cycle, were significantly downregulated. After exposure to drought stress for more than 4 days, the activities of four antioxidative enzymes (SOD, POD, CAT and APX) began to decrease and continued to decrease with longer stress exposure. Meanwhile, most of the genes encoding antioxidative enzymes were downregulated significantly. The downregulation of 21 genes related to the respiratory electron transport chain indicated that the blocked electron transfer accelerated excessive ROS. The MDA content was significantly elevated. The above data showed that 15 days of drought stress caused serious oxidative damage to *A. lancea*. Drought stress not only reduced the size and dry weight of *A. lancea*, but also lowered the amount of total volatile oil and the content of the main bioactive components. The total volatile oil and atractylodin content decreased slightly, whereas the content of atractylon and β -eudesmol decreased significantly. Moreover, ten significantly downregulated genes encoding sesquiterpene synthase were mainly expressed in rhizomes.

Conclusions: After exposed to drought stress, the process of assimilation was affected by the destruction of photosynthesis; stress tolerance was impaired because of the inhibition of the antioxidative enzyme system; and bioactive component biosynthesis was hindered by the downregulation of sesquiterpene synthase-related gene expression. All these had negative impacts on the quality formation of *A. lancea* under drought stress.

Keywords: *Atractylodes lancea* (Thunb.) DC, RNAseq, Photosynthetic rate, Antioxidative enzyme, Sesquiterpene, Gene expression, Quality formation

Background

Atractylodes lancea (Thunb.) DC, a perennial herb belonging to the Asteraceae family, has been listed as an endangered medicinal plant [1]. This medicinal herb has

*Correspondence: guwei2288@126.com

†Aqin Zhang and Mengxue Liu are co-first authors.

¹ School of Pharmacy, Nanjing University of Chinese Medicine, Nanjing 210000, China

Full list of author information is available at the end of the article



been traditionally used as an important crude drug for the treatment of digestive disorders, rheumatic diseases, night blindness, and influenza for a long time [2–5]. Besides that, it has been well proved that the active components from *A. lancea* exert great anti-cancer effect, especially in treatment of cholangiocarcinoma and gastric cancer [6–9]. Recently, it is interesting to find that *A. lancea* is frequently used in the treatment of Coronavirus Disease 2019 (COVID-19) and ranks first among the key Chinese herbal medicines for national epidemic prevention and control in China [10, 11]. So, there is an increasing demand of *A. lancea* with high quality. The main production areas in China (Jiangsu, Hubei, and Henan) have a temperate or subtropical climate, with aridity and little rain in spring and high temperature in summer; therefore, *A. lancea* often faces severe drought stress during its growth [12]. In addition, because of the scarcity of agricultural irrigation resources [13], artificial irrigation cannot be widely implemented to alleviate drought stress of *A. lancea*. Therefore, drought has become the main limiting factor affecting the quality formation of *A. lancea*.

The quality formation of medicinal plants is directly or indirectly influenced by the physiological state of plants [14]. Generally, plants with better physiological characteristics, such as more efficient photosynthesis and higher stress tolerance, can form better quality than plants with poor physiological traits [15, 16].

As the most basic and complex physiological process, photosynthesis is critical to all green plants. It is well established that drought stress can considerably influence plants' photosynthetic physiology by yellowing leaves, closing stomata, and weakening photosynthesis [17, 18]. The decreased photosynthetic capacity due to drought stress not only hampers the plant growth but also is directly/indirectly associated with the reduction of yield and quality in medicinal plants. Therefore, photosynthesis is a crucial and widely used physiological indicator to assess the influence of drought stress on the quality formation of medicinal plants [19]. However, there are still no reports about the photosynthetic response of *A. lancea* to drought stress. This hinders the understanding of the influence of drought stress on the quality formation of *A. lancea*.

It is generally believed that drought stress can induce excessive production of reactive oxygen species (ROS) which often disrupt the growth and quality formation of plants [20]. Antioxidative enzyme in plants is the major defense system to scavenge ROS for maintaining the normal physiological state of plants [21]. Thus, the high level of antioxidative enzyme activity is important for plants to tolerate stress for keeping good growth state and forming good quality. Generally, when plants

were subjected to drought stress, antioxidative enzymes' activities increased initially, but decreased with elevated drought stress level [22]. Zhou et al. [23] and Dai et al. [24] reported that short-term drought stress could induce the enhanced activities of antioxidant enzymes in *A. lancea* seedlings to reduce oxidative damage. This indicated that drought stress could affect the antioxidative enzyme activities of *A. lancea*. But, the plant material used in Zhou's and Dai's researches were *A. lancea* seedlings. So, it is essential to analyze the alteration of antioxidative enzyme activity in the adulted *A. lancea* exposed to drought stress for understanding of the influence of drought stress on the quality formation of *A. lancea*.

The oil content of *A. lancea* reaches about 2.02% to 4.06% [25]. The volatile oil, mainly composed of sesquiterpenes, is the main active substance of *A. lancea* and has liver-protective, analgesic, anti-viral, and gastrointestinal motility activities [2, 26, 27]. High levels of atractylon, β -eudesmol, and atractylodin are present in the volatile oil, and their levels are commonly used as indices to evaluate the quality of *A. lancea* [28]. Sesquiterpenes are mainly synthesized by the mevalonate (MVA) pathway in plants [29]. The universal precursor, farnesyl diphosphate (FPP), can be converted into different sesquiterpene skeletons by different sesquiterpene synthases (SSs) [30]. Previous studies showed that drought stress changed the content of sesquiterpenes in *Ocimum basilicum* L. by regulating the expression of key genes encoding enzymes of terpene biosynthesis [31]. Until now, some researches on the biosynthetic pathway of sesquiterpenes in *A. lancea* have been reported [32, 33], but, the effect of drought on accumulation and biosynthesis of sesquiterpenes in *A. lancea* is still unclear. Thus, it is essential to determine the accumulation of main bioactive component and to analyze expression level of genes related to sesquiterpene biosynthesis in *A. lancea* under drought stress. This will help us to understand the influence of drought stress on the quality formation of *A. lancea*.

The main research content of the present study was: 1. To establish a transcriptome database of *A. lancea* leaves and rhizomes under normal water management and under drought stress using DNA sequencing, and to verify the accuracy of the data using quantitative real-time reverse transcription PCR (qRT-PCR); 2. To study the effects of drought stress on the photosynthetic physiology of *A. lancea* by measuring chlorophyll content, photosynthesis parameters, and chlorophyll fluorescence (ChlF), and to analyze the expression levels of genes encoding important regulatory enzymes in photosynthesis; 3. To study the antioxidant ability of *A. lancea* under drought by measuring the activity of antioxidative enzymes and analyzing the expression levels of genes associated with antioxidative enzymes and 4. To study

the effect of drought stress on the yield and quality of *A. lancea* by determining the dry weight and the content of bioactive components and analyzing the expression levels of genes related to bioactive components' biosynthesis. Through the achievement of the above research content, we hope to provide a detailed understanding of the influence of drought stress on the quality formation of *A. lancea*. This will not only benefits for developing management strategy of *A. lancea* to minimize the quality reduction induced by drought, but also contributes to future drought tolerance breeding in *A. lancea*.

Results

Transcriptomic profiles, differentially expressed genes (DEGs) clustering analysis, and qRT-PCR validation

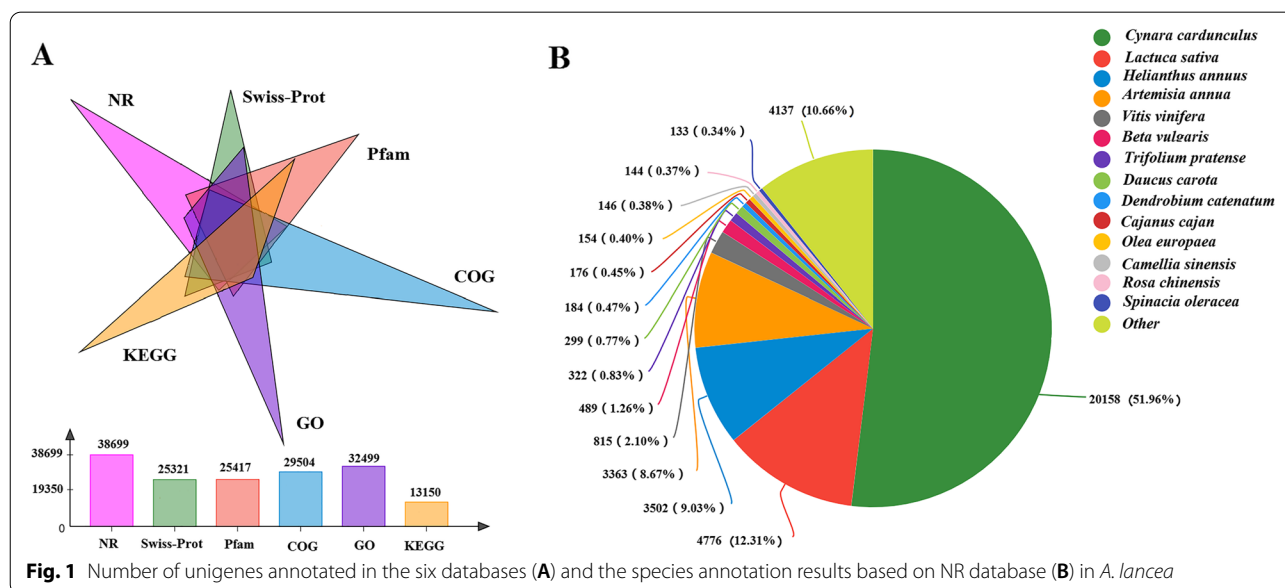
A total of 351,123,566 high-quality clean reads with a Q20 \geq 97.86% and a GC base ratio between 44.84% and 46.01% (Table S1) were generated. After assembling the clean reads, 82,677 unigenes and 14,0145 transcripts were obtained (Table S2). The detailed annotation results of the 82,677 unigenes were shown in Fig. 1A, and the top four similar species were *Cynara cardunculus* (51.96%), *Lactuca sativa* (12.31%), *Helianthus annuus* (9.03%), and *Artemisia annua* (8.67%) (Fig. 1B). These four species all belong to the Asteraceae family, as does *A. lancea*.

Using $p\text{-adjust} < 0.001$ and $|\log_2\text{FC}| \geq 1$, 30,510 DEGs were obtained between drought treatment (DT) group and control (CK) group. Using cluster analysis, these 30,510 DEGs could be divided into six clusters according to their pattern of gene expression. Cluster 1 contained 4160 DEGs that were downregulated in both leaves and rhizomes. Cluster 2 comprised 2714 genes whose

expression was downregulated in leaves, but was not significantly different in rhizomes. Cluster 3 contained 3377 genes that were downregulated in leaves and upregulated in rhizomes. Cluster 4 contained 6452 DEGs whose expression was downregulated in rhizomes but was not significantly different in leaves. Cluster 5 contained 6452 DEGs that were upregulated in leaves and downregulated in rhizomes. Cluster 6 contained 7480 genes that were upregulated genes in both leaves and rhizomes (Fig. 2A). GO functional enrichment analysis were performed on the DEGs in the six clusters (Fig. 2B). It is interesting that many DEGs in cluster 1 and cluster 5 were enriched in GO terms associated with redox processes, such as "oxidoreductase activity" (GO:0,016,901), "hydrogen peroxide metabolic process" (GO:0,042,743), and "monooxygenase activity" (GO:0,004,497). In addition, DEGs in cluster 3 were mainly enriched in GO terms related to photosynthesis, such as "chloroplast thylakoid membrane" (GO:0,009,535) and "photosynthetic membrane" (GO:0,034,357), and these genes are all downregulated in leaves, suggesting that the photosynthesis of *A. lancea* was inhibited by drought stress.

These 30,510 DEGs were also associated with 133 KEGG pathways (Figure S1), among which 100 pathways belonged to metabolism, accounting for the majority of DEGs. It is worth noting that three pathways were related to photosynthesis and five pathways were associated with terpenoid biosynthesis (Table 1).

The expression levels of five selected genes (*DN15090_c0_g1*, *DN474_c1_g1*, *DN18330_c1_g1*, *DN47389_c0_g1*, and *DN54795_c0_g2*) calculated using qRT-PCR were listed in Table S3. The gene expression trends were



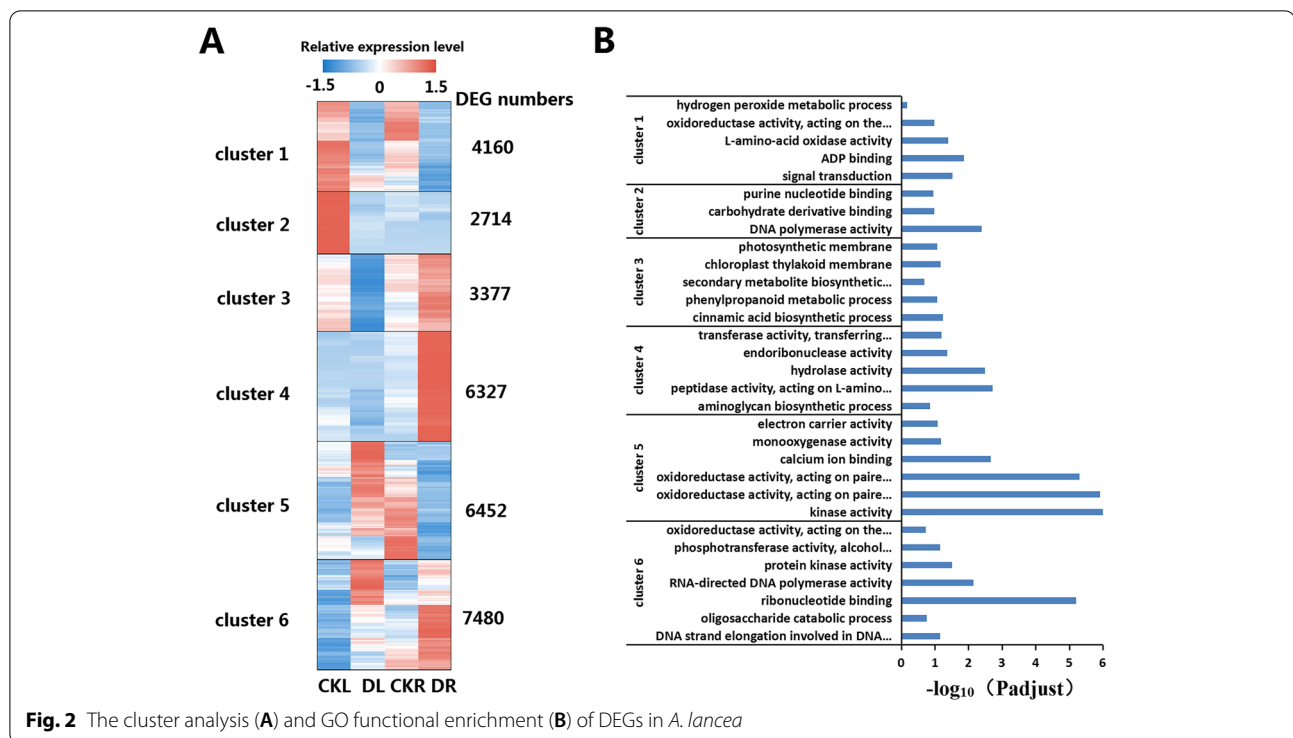


Table 1 Pathways related to photosynthesis and terpenoid biosynthesis

pathway ID	Description	Number of DEGs
map00195	Photosynthesis	18
map00196	Photosynthesis—antenna proteins	6
map00710	Carbon fixation in photosynthetic organisms	51
map00909	Sesquiterpenoid and triterpenoid biosynthesis	26
map00900	Terpenoid backbone biosynthesis	27
map00904	Diterpenoid biosynthesis	14
map00902	Monoterpenoid biosynthesis	25
map01062	Biosynthesis of terpenoids and steroids	1

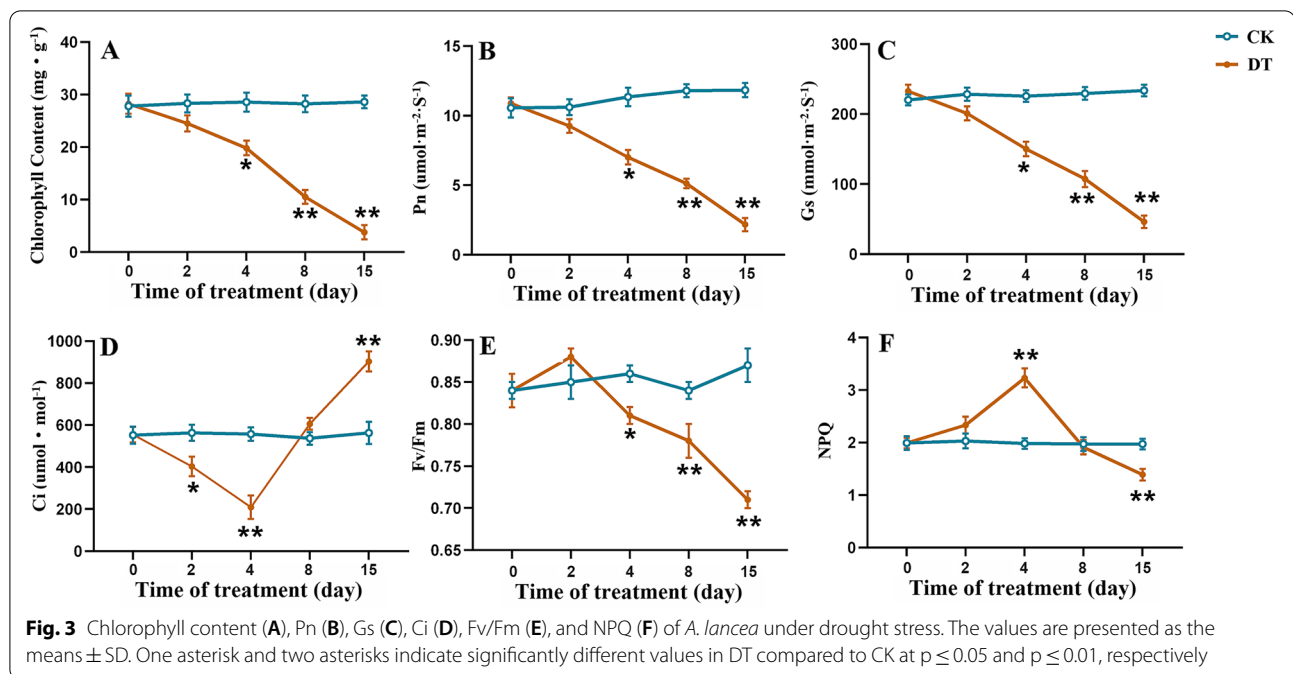
consistent with those in the transcriptome sequencing data, confirming that the transcriptome-based DEG results were reliable to identify drought-responsive genes in the present study.

Changes in the photosynthesis system and associated gene expression analysis

Under drought stress, all of the measured photosynthesis parameters of *A. lancea* showed obvious alterations. As the duration of drought stress treatment increased, the chlorophyll (CHL) content, net photosynthesis (Pn) and stomatal conductance (Gs) of *A. lancea* all showed continuous downward trends (Fig. 3A-3C). On the 15th of

treatment, the values of CHL, Pn and Gs in the DT group were significant smaller than those in the CK group. The intercellular carbon dioxide concentration (C_i) of *A. lancea* started to decrease within 4 days of drought treatment and then began to increase from the 5th day of drought stress treatment, leading to a higher final C_i in the DT group (Fig. 3D). As for chlorophyll fluorescence, drought stress caused a significant reduction in the potential yield of the photochemical reaction of PsII (Fv/Fm) and the longer the drought stress, the greater the reduction (Fig. 3E). The value of non-photochemical quenching (NPQ) also altered significantly as the prolonged drought treatment, increased on the first 4 days, and then decreased from the 5th day (Fig. 3F).

To gain a deeper understanding of the mechanisms underlying the reduced photosynthesis of *A. lancea* under drought stress, 31 DEGs encoding key enzymes participating in the light and dark reactions of photosynthesis were identified in leaves. Among these 31 DEGs, 11 were upregulated and 20 were downregulated. In total, among seven DEGs involved in the light reaction (Fig. 4A), *DN31152_c0_g2* (F-type H^+/Na^+ ATP synthase gene) and *DN1739_c0_g1* (photosystem I P700 apoprotein A1 gene) were upregulated. The other five downregulated DEGs associated with the light reaction were *DN21336_c0_g1* (photosystem I P700 apoprotein A1 gene), *DN19968_c0_g1* and *DN32471_c0_g1* (F-type H^+/Na^+ ATP synthase gene), *DN18889_c0_g1*



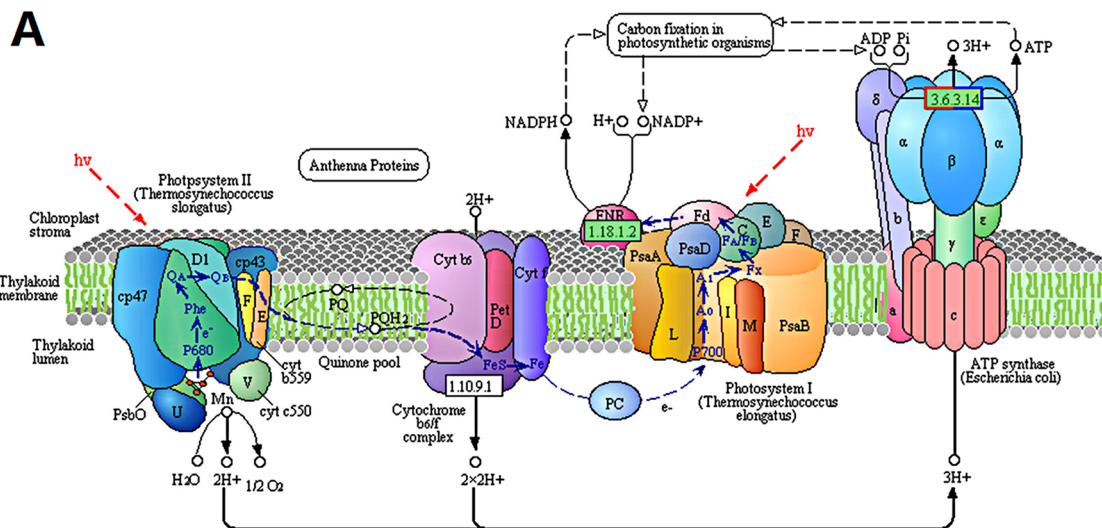
(photosystem II CP47 reaction center protein gene), and *DN60086_c0_g1* (photosystem II reaction center W protein gene). Twenty-four DEGs were involved in dark reaction, among which 9 DEGs were upregulated and 15 were downregulated (Fig. 4B). The upregulated 9 DEGs included five malate dehydrogenase genes (*DN7011_c0_g1*, *DN18398_c0_g1*, *DN48988_c0_g1*, *DN69445_c0_g1* and *DN39038_c0_g1*), a glyceraldehyde-3-phosphate dehydrogenase gene (*DN1992_c4_g1*), a ribose-5-phosphate isomerase gene (*DN1163_c0_g2*), a phosphoglycerate kinase gene (*DN34957_c0_g1*) and a pyruvate, phosphate dikinase gene (*DN23841_c0_g1*). The 15 downregulated DEGs included six malate dehydrogenase genes (*DN1618_c0_g2*, *DN45011_c0_g1*, *DN3381_c1_g1*, *DN16280_c0_g1*, *DN61455_c1_g1*, and *DN17392_c0_g1*), two triosephosphate isomerase genes (*DN7162_c3_g1* and *DN24632_c0_g2*), a ribulose biphosphate carboxylase gene (*DN1343_c0_g2*), a glyceraldehyde-3-phosphate dehydrogenase gene (*DN4492_c0_g3*), an alanine aminotransferase gene (*DN14431_c0_g1*), a pyruvate, phosphate dikinase gene (*DN4030_c0_g2*), a phosphoglycerate kinase gene (*DN9649_c0_g1*), a phosphoenolpyruvate carboxykinase gene (*DN3731_c0_g1*), and a fructose-1,6-bisphosphatase gene (*DN39571_c0_g2*).

Changes in the protective enzymes system and associated gene expression analysis

The activities of SOD, POD, CAT and APX were higher in the DT group than those in the CK group during the early stage of drought stress. For SOD and POD, the

early stage of drought stress was 0 to 8 days. For CAT and APX, it was 0 to 4 days. After the early stage, the activities of these enzymes began to decrease. On the 15th day of drought stress, the activity of the four antioxidant enzymes were all different with those in the CK group. The activities of SOD and APX in the DT group were significantly lower than those in the CK group. The POD activity was significantly higher than that in the CK group and CAT activity is slightly (non-significantly) lower than that in the CK group (Fig. 5A-5D). In addition, the amount of MDA increased rapidly in *A. lancea* under drought stress, while there was no change in MDA levels in the CK group (Fig. 5E). The relative conductivity showed a similar result to the MDA content (Fig. 5F).

The detailed analysis of transcriptome of *A. lancea* under normal water management and under drought stress provided a large number of DEGs encoding antioxidant enzymes. There were five SOD genes (*DN3525_c0_g1*, *DN19179_c0_g3*, *DN19917_c0_g1*, *DN474_c1_g1*, and *DN53562_c0_g1*) and ten CAT genes (*DN5539_c0_g4*, *DN42828_c0_g1*, *DN3870_c0_g1*, *DN49828_c0_g1*, *DN9135_c1_g1*, *DN5359_c0_g1*, *DN3848_c0_g1*, *DN7441_c0_g1*, *DN25688_c0_g1*, and *DN3848_c0_g2*). These 15 DEGs were all downregulated under drought stress. In addition, 18 POD genes were obtained, including six upregulated DEGs (*DN21191_c0_g1*, *DN4672_c0_g2*, *DN51705_c0_g1*, *DN35661_c0_g1*, *DN2622_c1_g1*, and *DN18330_c1_g1*) and 12 downregulated DEGs (*DN838_c0_g1*, *DN68449_c0_g1*, *DN7681_c1_g1*, *DN75393_c0_g2*, *DN9309_c0_g2*,



Photosystem II

D1	D2	cp43	cp47	cyt b559		
PsbA	PsbD	PsbC	PsbB	PsbE	PsbF	
MSP OEC						
PsbL	PsbJ	PsbK	PsbM	PsbH	PsbI	PsbO
PsbQ	PsbR	PsbS	PsbT	PsbU	PsbV	PsbW
PsbY	PsbZ	Psb27	Psb28	Psb28-2		

Photosystem I

PsaA	PsaB	PsaC	PsaD	PsaE	PsaF	PsaG	PsaH
PsaI	PsaJ	PsaK	PsaL	PsaM	PsaN	PsaO	PsaX

F-type ATPase

beta	alpha	gamma	delta	epsilon	c	a	b
------	-------	-------	-------	---------	---	---	---

Item	DEGs
Psb B	<i>DN18889_c0_g1</i>
Psb W	<i>DN60086_c0_g1</i>
Psa A	<i>DN21336_c0_g1</i>
Psa B	<i>DN1739_c0_g1</i>
beta	<i>DN31152_c0_g2; DN32471_c0_g1</i>
delta	<i>DN19968_c0_g1</i>

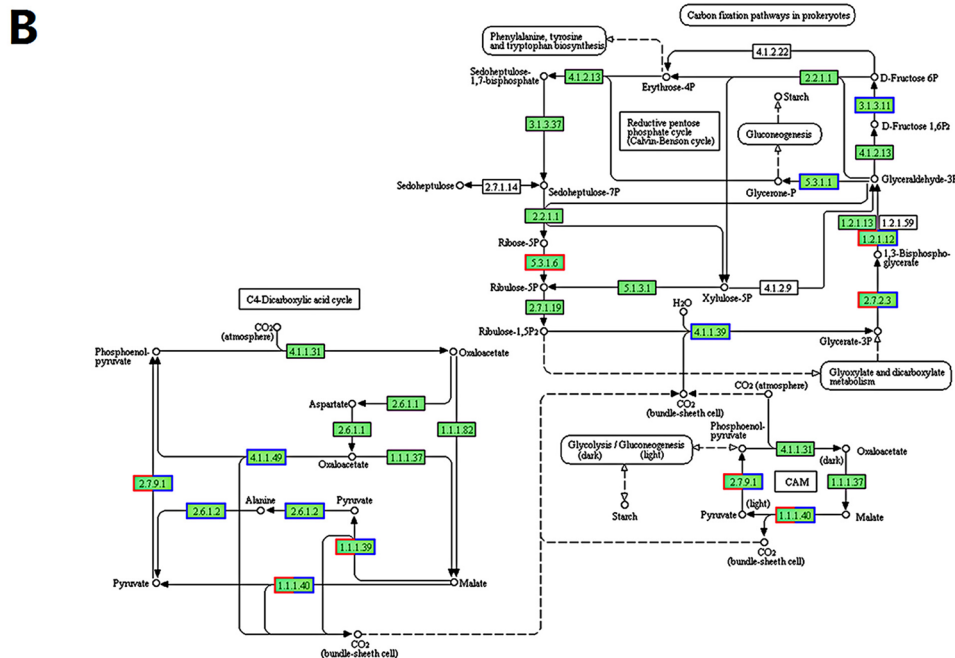
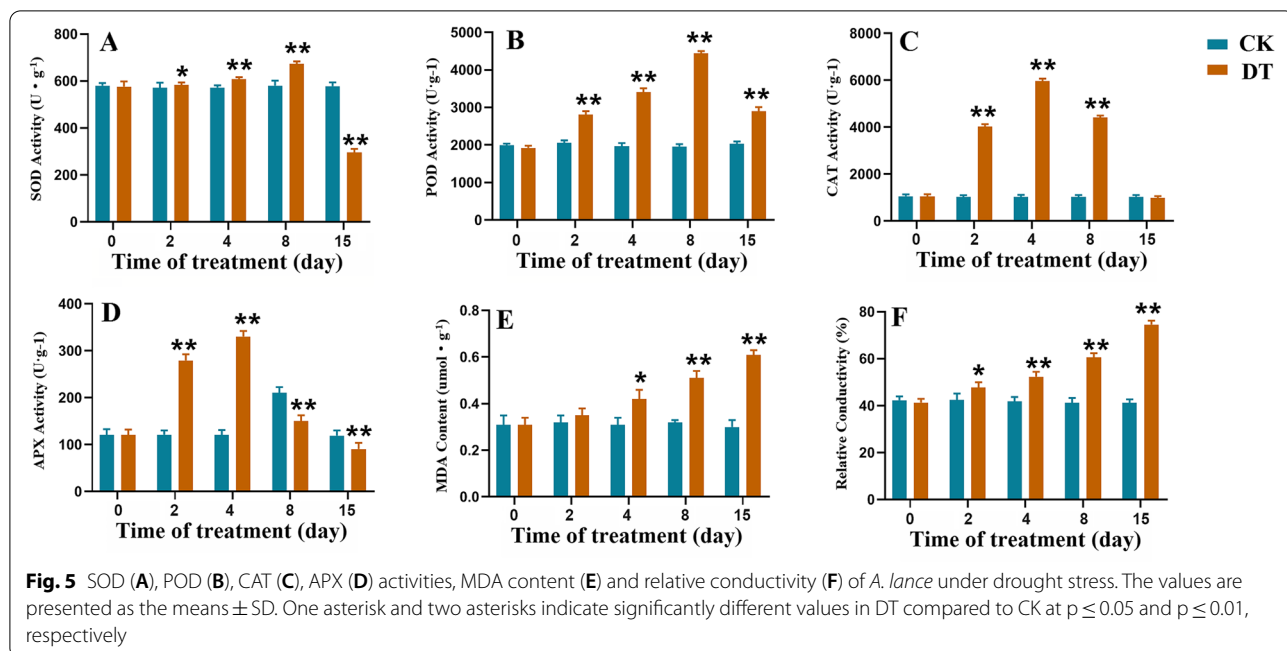


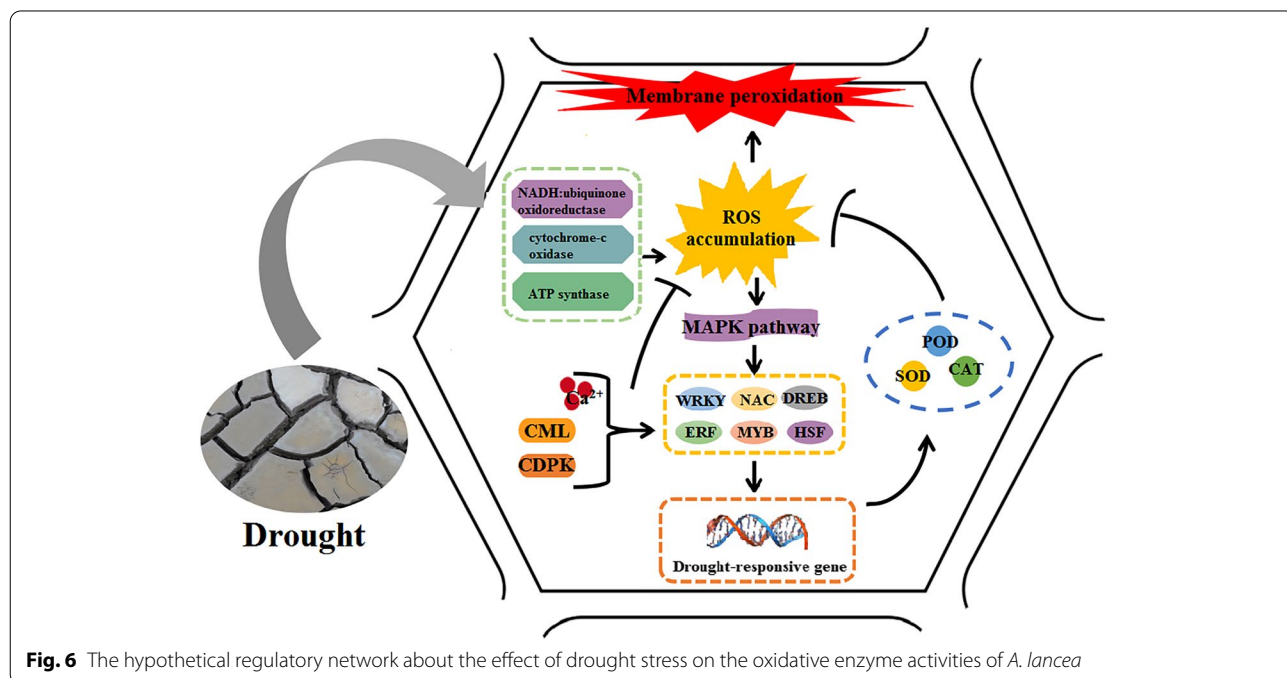
Fig. 4 DEGs involved in light reaction (A) and dark reaction (B) of photosynthesis



DN40830_c0_g1, *DN52474_c0_g4*, *DN42408_c0_g1*, *DN61971_c0_g1*, *DN45395_c0_g1*, *DN19722_c0_g2*, and *DN15530_c0_g3*.

It has been reported that ROS can act as second messengers to transduce the signal to transcription factors, thus in turn activate gene expression of antioxidative enzymes. So, we also paid attention to DEGs associated

with ROS production and found that 21 downregulated DEGs were related to the respiratory electron transport chain under drought stress (Fig. 6). The 21 DEGs comprised four NADH: ubiquinone oxidoreductase genes (*DN215_c1_g1*, *DN13447_c0_g2*, *DN5922_c2_g2*, and *DN30220_c0_g1*), two cytochrome-c oxidase genes (*DN7184_c0_g1* and *DN26312_c0_g1*), and 15



ATP synthase genes (*DN7129_c0_g1*, *DN1539_c0_g1*, *DN1467_c0_g1*, *DN19968_c0_g1*, *DN5265_c0_g1*, *DN14586_c0_g1*, *DN4776_c0_g1*, *DN32471_c0_g1*, *DN5303_c1_g2*, *DN2129_c1_g1*, *DN2238_c0_g2*, *DN1584_c1_g3*, *DN17811_c0_g1*, *DN27345_c0_g1* and *DN77850_c0_g1*).

Changes in bioactive component contents and associated gene expression analysis

The rhizomes of *A. lancea*, sampled after 15 days of drought stress treatment, were used as the experimental materials for quality assessment. Morphologically, the rhizomes of *A. lancea* from the DT group were smaller than those from the CK group (Fig. 7A). Moreover, drought stress treatment led to a reduction in the dry weight of *A. lancea* rhizomes. The average dry weight of the rhizomes from the DT group was 7.85 ± 2.01 g, while the average dry weight of the rhizomes from the CK group was 14.23 ± 4.16 g. The proportion of essential oil also showed difference between the two groups. The essential oil content of *A. lancea* in the CK and DT group was 0.111 ml/g and 0.096 ml/g, respectively. In addition, the content of three bioactive components (atractylon, β -eudesmol, and atractylodin) all showed decreasing

trends in *A. lancea* in the DT group compared with that in the CK group (Fig. 7B). Importantly, the amount of atractylon decreased significantly ($P < 0.05$). Notably, a sharp reduction ($P < 0.01$) was observed in the content of β -eudesmol.

We next turned our attention to DEGs associated with “terpenoid backbone biosynthesis” (map00900) and “sesquiterpenoid and triterpenoid biosynthesis” (map00909) and identified 18 DEGs associated with sesquiterpenoid biosynthesis. Among them, eight DEGs were related to the MVA pathway, including two hydroxymethylglutaryl-CoA synthase genes (*DN8392_c0_g1* and *DN2865_c0_g3*), four hydroxymethylglutaryl-CoA reductase genes (*DN48911_c0_g2*, *DN1889_c2_g2*, *DN86031_c0_g1*, and *DN16497_c0_g1*), and two diphosphomevalonate decarboxylase genes (*DN79187_c0_g1* and *DN23531_c0_g1*). Under drought stress, some of these 8 genes were upregulated and some were downregulated, i.e., they did not show a consistent pattern. In addition, 10 DEGs associated with sesquiterpene synthase were obtained. Among them, seven (*DN56449_c0_g2*, *DN2689_c0_g2*, *DN1597_c0_g1*, *DN54795_c0_g2*, *DN18787_c0_g2*, *DN1159_c0_g1*, and *DN3448_c0_g2*) were significantly downregulated (Fig. 8) and three (*DN18629_c0_g2*, *DN18787_c0_g1*, and

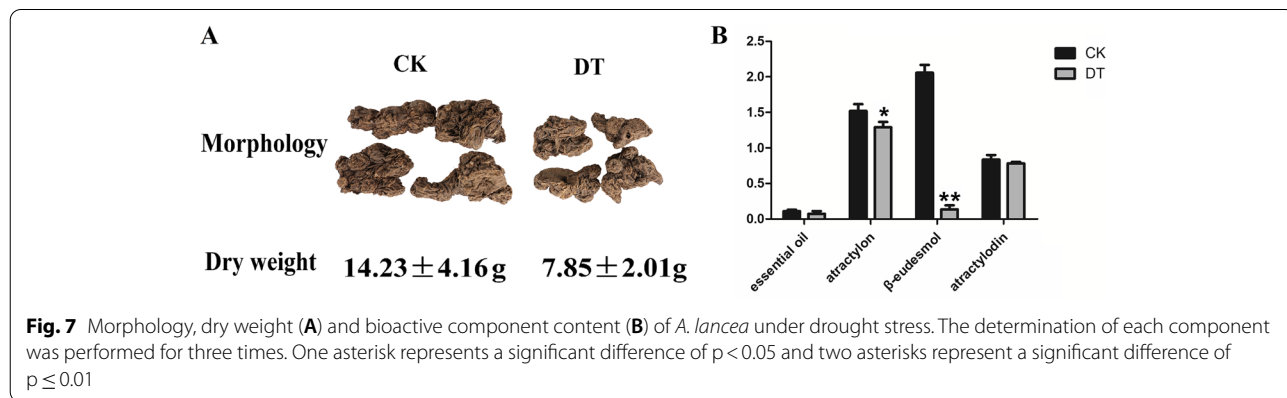


Fig. 7 Morphology, dry weight (A) and bioactive component content (B) of *A. lancea* under drought stress. The determination of each component was performed for three times. One asterisk represents a significant difference of $p < 0.05$ and two asterisks represent a significant difference of $p \leq 0.01$

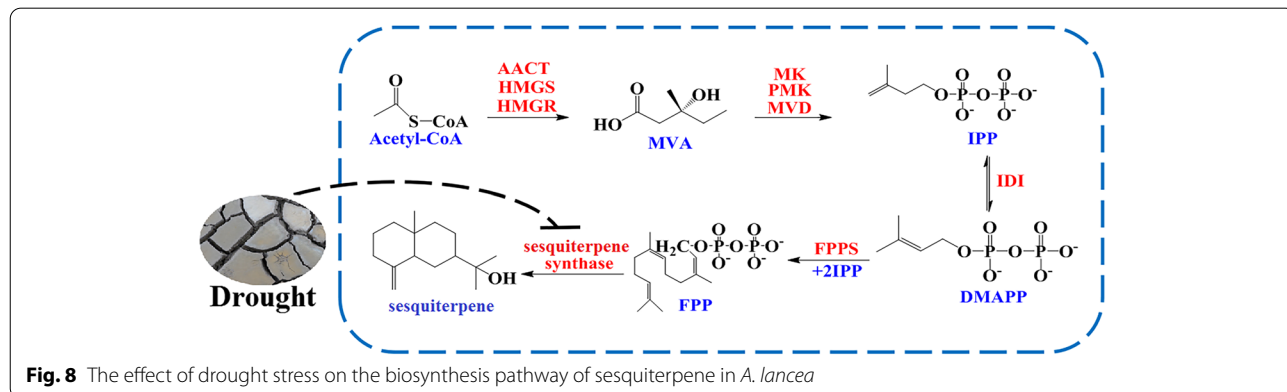


Fig. 8 The effect of drought stress on the biosynthesis pathway of sesquiterpene in *A. lancea*

DN85030_c0_g1) were upregulated. These sesquiterpene synthase genes were mainly differentially expressed in rhizomes (n = 8) with only two expressed in leaves.

Discussion

The quality formation of medicinal plant is an extreme complex process which was mainly determined by two aspects: heredity and environment [34]. Certainly, suitable environment is quite important for the quality formation of medicinal plants [35]. However, with the deterioration of the global climate, encountering drought stresses has been more common and frequent during medicinal plants' growth. Thus, drought has become a crucial limiting factor that influence the quality formation of medicinal plants [36, 37]. In present study, the effect of drought stress on the quality formation of *A. lancea* was studied by analyzing photosynthesis, antioxidative enzyme activity and bioactive component accumulation.

Photosynthesis is particularly sensitive to drought stress and often is inhibited because of stomata closure induced reduced CO₂ supply and further metabolic impairment by drought stress [38, 39]. Generally, the total dry matter production of a plant is equal to its net photosynthesis [40]. So, drought stress causes a reduction of photosynthesis rates in medicinal plants, leading to low yields of medicinal plants. In present study, the significant decrease of Pn in *A. lancea* from the DT group confirmed that drought stress lasted for 15 days caused obvious photosynthesis inhibition in *A. lancea*. This result was consistent with previous studies [41, 42]. The continuous declined Gs indicated that limitations of CO₂ uptake caused by stomata closure was responsible for photosynthesis inhibition [43]. With prolonged drought stress, Ci began to increase, suggesting that metabolic impairment induced by drought became another main limiting factor. Rubisco (ribulose biphosphate carboxylase) is the key enzyme participated in the first stage of the Calvin cycle by catalyzing ribulose-1,5-bisphosphate and CO₂ to form two molecules of 3-phosphoglyceric acid (3-PGA) [44]. In the present study, A Rubisco gene (*DN1343_c0_g2*) was significantly downregulated under drought stress, indicating that drought stress caused metabolic impairment in *A. lancea* by inhibiting the carboxylation reaction of CO₂. The rate of photosynthesis also depends on the regeneration of RuBP [45]. Fructose-1,6-bisphosphatase (FBP) and triosephosphate isomerase (TPI) can catalyze glyceraldehyde-3-phosphate (GAP) through a series of transformations to reform RuBP [46, 47]. A FBP gene (*DN39571_c0_g2*) and two TPI genes (*DN7162_c3_g1* and *DN24632_c0_g2*) were significantly downregulated, indicated that drought stress could also

cause metabolic impairment in *A. lancea* by hindering the regeneration of RuBP.

The Fv/Fm ration represent the potential yield of the photochemical center of photosystem II (PSII) [48]. The value of Fv/Fm ration has been reported to stay around 0.83 among many different plant species under normal growth conditions [49]. When the plant was exposed to drought stress, Fv/Fm is particularly sensitive and its value decreased greatly [50]. Thus, Fv/Fm has already become an important parameter to judge the physiological state of plants under drought stress. In present study, the Fv/Fm value of *A. lancea* in the CK group was kept at a relative stable level, while the Fv/Fm in the DT group showed a significantly reduction. This demonstrated that the efficiency of light energy conversion and electron transfer activities were all markedly inhibited under drought stress. The characteristic decrease of Fv/Fm induced by drought stress was consistent with previous studies [51, 52]. The reduction in Fv/Fm is often associated with an increase in the efficiency of non-photochemical quenching (NPQ) [53]. Under drought stress, the significantly increased NPQ showed that excessive irradiation could be dissipated into heat to protect *A. lancea* from drought-induced damage. The observed reduction in efficiency of PSII was concomitant with the down-regulation of genes belonging to the PSII category induced by drought stress, evidencing that the reduced efficiency of PSII was the other main limiting factor of photosynthesis inhibition in *A. lancea* under drought stress.

Combined with the lower dry weight of *A. lancea* under drought stress, we inferred that drought inhibited photosynthesis of *A. lancea* by closing stomata, reducing the CHL content, limiting the efficiency of PSII and inducing metabolic impairment, which led to a yield decline, thereby affecting the quality formation of *A. lancea*.

Drought stress inevitably causes excessive production of ROS, which can oxidize biofilms, form lipid peroxidation products, and damage cells [54]. Antioxidative enzymes form the first line of defense against ROS and have been reported to contribute directly or indirectly in drought tolerance of many plants, such as rice [55], alfalfa [56] and canola [57]. Adebayo (2015) stated that sustained yields in maize under drought stress were directly related to better antioxidant activities [58]. In present study, the activities of SOD, POD, CAT and APX were higher in the DT group than those in the CK group during the early stage of drought stress. This was consistent with Zhou's and Dai's researches. This implied that during the early stage of drought stress, ROS acted as second messengers involved in the stress signal transduction pathway to activate antioxidative enzyme activity. Like other plants, the induction of antioxidant enzyme activity

is an adaptation strategy which *A. lancea* use to overcome oxidative stresses. The balance between ROS production and activities of antioxidative enzymes determined whether oxidative signaling and/or damage would occur [59]. As the duration of drought treatment increased, the activities of all four antioxidative enzymes decreased. On the 15th day, except for POD, the activities of SOD, CAT and APX were lower compared with those in the CK group. And gene expression analysis identified 35 antioxidant enzyme genes and 26 of them were significantly downregulated under 15 days' drought stress. This may reflect the low ROS scavenging capacity and increased damage in *A. lancea* under 15 days' drought stress. The decrease of antioxidant enzyme activity under progressive drought stress also has been reported by many previous studies. In addition, 21 significantly downregulated genes related to the respiratory electron transport chain in *A. lancea* under drought stress, suggested that the blocked electron transport would accelerate the accumulation of ROS [60]. So, it could be concluded that the level of ROS induced by 15 days of drought stress in *A. lancea* was beyond the adjustable range of the plant itself, and the antioxidative enzyme system could no longer remove the excessive ROS. The markedly elevated level of MDA and relative conductivity under drought stress also evidenced the severe oxidative damage to *A. lancea* caused by drought stress. Taken together, our data suggested that the significant decline of antioxidative enzyme activity was an important factor affecting *A. lancea*'s stress tolerance, thereby affecting the quality formation of *A. lancea*.

The amount of volatile oil and the content of atractylon, β -eudesmol, and atractylodin are often used as indices to evaluate the quality of *A. lancea* [28]. In present study, not only the amount of volatile oil, but also the content of atractylon, β -eudesmol, and atractylodin decreased in *A. lancea* under drought stress. This confirmed that 15 days' drought stress negatively affected the quality of *A. lancea*. Expression analysis of genes related to sesquiterpene biosynthesis provided 18 DEGs. Although there was not a consistent pattern about the expression regulation of DEGs involved in the upstream of sesquiterpene biosynthesis, seven DEGs encoding sesquiterpene synthase, a key regulatory enzyme in the downstream of sesquiterpene biosynthesis were significantly downregulated. This suggested that drought stress could reduce the accumulation of sesquiterpene components by reducing the expression levels of associated sesquiterpene synthase genes. Overall, the downregulated gene expression of sesquiterpene synthase and the low amounts of volatile oil, atractylon, β -eudesmol, and atractylodin illustrated that drought stress slowed down the bioactive components' biosynthesis and accumulation, thereby affecting the quality formation of *A. lancea*.

Conclusions

Drought stress affected the quality formation of *A. lancea* from the following three aspects. First, genes encoding important regulatory enzymes in dark reaction were downregulated significantly, the efficiency of PSII was limited, thus, photosynthesis was significantly inhibited. Second, gene expression and activities of antioxidative enzymes were mostly downregulated, thus, the stress tolerance of *A. lancea* was impaired. Third, gene expression of key enzymes involved in sesquiterpene biosynthesis were down-regulated, thus, the accumulation of bioactive components was slowed down in *A. lancea*.

Methods

Plant materials and drought stress treatment

A. lancea was obtained from Maoshan (N31°79'14.98", E119°32'19.56"), Jurong, Jiangsu Province, China and identified as *Atractylodes lancea* (Thunb.) DC by Professor Wei Gu (School of Pharmacy, Nanjing University of Chinese Medicine, China). The voucher was deposited in Department of Chinese Medicine Resources, Nanjing University of Chinese Medicine with ID MCZ-19-001. The *A. lancea* used in the present study were artificially cultivated, so, there was no permission needed for the collection of *A. lancea*. Then the plants were transplanted in the Medicinal Botanical Garden, Nanjing University of Traditional Chinese Medicine (NUTCM). Five *A. lancea* plants were in a plastic pot (top diameter 38 cm, bottom diameter 32 cm, height 35 cm) with approximately 20 kg dry soil. The potted plants were grown in a greenhouse with 25 °C, 60% relative humidity and 14 h of light and 10 h of darkness. Soil taken from the Medicinal Botanical Garden of NUTCM was air-dried naturally and then passed through a 5 mm sieve. The experimental soil was prepared by mixing the air dried soil and farmyard manure evenly in a ratio of 4:1. The detailed information of the prepared experimental soil was as followed: texture, loam; organic matter, 12.74 g/kg; total nitrogen, 2.12 g/kg, total phosphorous, 3.57 g/kg; total potassium, 12.53 g/kg; alkalihydro nitrogen, 63.38 mg/kg; available phosphorus, 20.53 mg/kg; available potassium, 49.86 mg/kg; pH, 6.52. After adaption for two weeks, sixty *A. lancea* plants with similar growth rates were randomly divided into two groups: CK group and DT group. Soil water content was measured using a TZS-IIW Soil Moisture Meter (Zhejiang Top Instrument Co., Ltd, Zhejiang, China). The water content was kept at 55% to 65% and 25% to 35% of saturated soil water content in the CK group and the DT group for 15 days, respectively. At 0, 2, 4, 8, and 15 days of the stress treatment, leaves of the two groups were collected and divided into two parts. One part was used for physiological index measurements and

the other part was immediately frozen in liquid nitrogen for RNA extraction. In addition, the rhizomes of the two groups were collected at 0, 2, 4, 8, and 15 days and were also divided into two parts. One half of each sample was frozen in liquid nitrogen to be used for RNA extraction, and the other half was oven-dried at 40 °C to a constant weight for quality analysis.

Illumina sequencing and functional annotation

Leaves and rhizomes of the two groups collected at 15 days were used to isolate total RNA using an RNeasy Plus Mini Kit (#74,134; Qiagen, Hilden, Germany). The cDNA was synthesized using the fragmented mRNA as a template. PCR amplification was then performed, and then high-throughput sequencing was performed on a Illumina HiSeq TM 4000 instrument by Shanghai Megi Biomedical Technology Co., Ltd (Shanghai, China). Fastx_toolkit_0.0.14 (http://hannonlab.cshl.edu/fastx_toolkit/) was used for quality assessment of the raw sequencing data. After obtaining high-quality clean reads. Trinity_v2.8.5 (<https://github.com/trinityrnaseq/trinityrnaseq>) was used to assemble the clean reads into transcript sequences, and TransRate (<http://hibberdlab.com/transrate>) was applied to filter the transcripts. The optimized transcript sequences were stored as FASTQ files under the project accession numbers (SRR8699030, SRR8699031, SRR8699032, and SRR8699033) in the Short Read Archive database of the NCBI.

Gene annotation information was obtained by BlastX searching in the NCBI non-redundant protein database (NR, <http://www.ncbi.nlm.nih.gov>), and by analysis using the following database resources: Cluster of Orthologous Groups (COG), Swissprot (<http://www.expasy.ch/sprot>), Kyoto Encyclopedia of Genes and Genomes (KEGG, <http://www.genome.jp/kegg>), Pfam (<http://pfam.xfam.org/>), and Gene Ontology (GO, <http://www.geneontology.org>). The E-value was set to $1E^{-5}$.

Gene expression analysis and qRT-PCR validation

Gene expression was calculated using RSEM (<http://deweylab.github.io/RSEM/>) and normalized by the FPKM (Fragments per Kilobases per Million reads) value. EdgeR_3.24.3 (<http://bioconductor.org/packages/stats/bioc/edgeR/>) were used to obtain DEGs, and Bonferroni one-step correction was used as a multiple test correction method, and $p\text{-adjust} < 0.05$ and $|\log_2\text{fold-change (FC)}| \geq 2$ were used as criteria. Fisher's exact test was used for DEG enrichment analysis. When the false discovery rate (FDR) was < 0.05 , the GO function item or the KEGG pathway was considered to be significantly enriched for the DEG.

Expression levels of five randomly selected genes (*DN15090_c0_g1*, *DN474_c1_g1*, *DN18330_c1_g1*,

DN47389_c0_g1, and *DN54795_c0_g2*) were analyzed to validate the accuracy of transcription sequencing results. The qRT-PCR reaction was performed according to the Platinum® SYBR® Green qPCR Supermix UDG real-time PCR kit instructions (Thermo Fisher Scientific, Waltham, MA, USA). The qPCR reaction comprised: Pre-denaturation at 94 °C for 5 min, followed by 40 cycles of denaturation at 94 °C for 30 s, annealing at 62 °C for 30 s, and extension at 72 °C for 40 s. *EF1A1* (encoding EF-1 α) was used as an internal reference gene, and the $2^{-\Delta\Delta C_t}$ method was used to calculate the relative expression level of a gene. The experiment was performed three times, and each sample was assessed three times. The specific qPCR primers were designed using Primer Premier 5.0 software (PREMIER Biosoft International, San Francisco, CA, USA) and were supplied by Generay Biotech Co., Ltd. (Shanghai, China; Table S4).

Photosynthesis measurement

An LI-6400XT photosynthesis-fluorescence measurement system was applied to measure photosynthesis and chlorophyll fluorescence parameters. The determination of net photosynthesis (Pn), stomatal conductance (Gs), and the intercellular carbon dioxide concentration (Ci) were carried out between 9:00 and 11:00 in the morning. After being subjected to dark adaptation treatment for 2 h from 12 noon, the plants were subjected to photochemical efficiency measurement to obtain the Fv/Fm (the ratio of variable to maximum fluorescence). Then, after 1 h of light activation, non-photochemical quenching (NPQ) was measured. The content of CHL was determined using Arnon's method [61].

Protective enzyme activity

The content of MDA was measured using the thiobarbituric acid method [62]. A conductivity meter, BDS-6300 (Shanghai Yidian Scientific Instrument Co., Ltd. Shanghai, China), was used to determine the relative conductivity. The riboflavin-trinitrotoluene chloride (NBT) method and guaiacol method were applied to detect SOD and POD activity [63]. The activities of CAT and APX were determined using a UV spectrophotometer UV 5200 (Shanghai Metash Instruments Co., Ltd. Shanghai, China) at 240 nm and 290 nm, respectively [62].

Determination of bioactive components

Essential oil was collected by steam distillation according to the volatile oil extraction method in the 2020 edition of the Chinese Pharmacopoeia [64].

A Waters e2695 series high performance liquid chromatography (HPLC) system (Waters Technology (Shanghai) Co. Ltd., Shanghai, China) was employed to analyze the samples. A Welchrome C₁₈ analytical column

(250 mm × 4.6 mm, 5 mm; Shanghai Welch Technology Co. Ltd., Shanghai, China) was used and the mobile phase was acetonitrile (A) and 0.1% v/v formic acid solution (B) at a flow rate of 1 mL·min⁻¹. The gradient was as follows: 0–5 min, 10% A, 5–6 min, 14% A, 6–22 min, 30% A, 22–27 min, 52% A, 27–55 min, 80% A, 55–65 min, 100% A. The column temperature was 30 °C and the injection volume was 10 µL. The detection wavelength was 340 nm for atracylodin and 203 nm for atractylon and β-eudesmol, respectively. The reference standards of atracylodin, atractylon, and β-eudesmol were purchased from Shanghai Yuanye Bio-Technology Co., Ltd (Shanghai, China).

Four hundred milligrams of rhizome sample powder and 10 mL of methanol were placed together in a brown triangular bottle and weighted precisely. After ultrasonic extraction for 40 min and cooling to room temperature, methanol was added to the mixture to make up for weight loss. Then, the supernatant was passed through a 0.45-µm micro-porous membrane to prepare the sample solution for HPLC analysis.

Statistical analysis

All data were assessed for significant differences ($P < 0.05$) using one-way analysis of variance (ANOVA) with Bonferroni correction using SPSS 20.0 software (IBM Corp., Armonk, NY, USA). Each experiment was performed three times independently and all data were presented as the mean and standard deviation (SD). The GraphPad Prism 8 (GraphPad Software, San Diego, CA, USA) was used to construct graphs.

Abbreviations

SOD: Superoxide dismutase; POD: Peroxidase; CAT: Catalase; APX: Ascorbate peroxidase; COVID-19: Coronavirus Disease 2019; AsA-GSH: Ascorbate–glutathione; MDA: Malondialdehyde; MVA: Mevalonate; FPP: Farnesyl diphosphate; SS: Sesquiterpenes synthase; QRT-PCR: Quantitative real-time reverse transcription PCR; DEG: Differentially expressed gene; DT: Drought treatment; NR: NCBI non redundant protein database; COG: Cluster of Orthologous Groups; KEGG: Kyoto Encyclopedia of Genes and Genomes; GO: Gene Ontology; ROS: Reactive oxygen species; CHL: Chlorophyll; Rubisco: Ribulose biphosphate carboxylase; Fv/Fm: The potential yield of the photochemical reaction of PsII; NPQ: Non-photochemical quenching; 3-PGA: 3-Phosphoglyceric acid; FBP: Fructose-1,6-bisphosphatase; TPI: Triosephosphate isomerase; GAP: Glyceraldehyde-3-phosphate.

Supplementary Information

The online version contains supplementary material available at <https://doi.org/10.1186/s12870-021-03048-9>.

Additional file 1: Table S1. Summary of RNA-Seq database from *A.lancea* under drought stress. **Table S2.** The detailed information for assembled unigenes of *A.lancea* under drought stress. **Table S3.** QRT-PCR validation of DEGs from *A.lancea*. **Table S4.** The primer list of DEGs for qRT-PCR validation. **Figure S1.** Functional classification for assembled unigenes of *A.lancea* by KEGG.

Acknowledgements

Not applicable.

Authors' contributions

AZ and ML conducted the experiments, performed the data analysis, and wrote the manuscript; ZC, YG, LP, and RT assisted in the data analysis; WG supervised the experiment, and led the data analysis and writing of the manuscript. All authors read and approved the final manuscript.

Funding

This research was supported by the National Natural Science Foundation of China (81573520), Administration of Subsidy Funds for Public Health Services of traditional Chinese Medicine "National survey of traditional Chinese Medicine resources" [Ministry of Finance (2019) 39] and the Natural Scientific Fund of the Jiangsu Higher Education Institutions of China (No. 18KJB360012).

Availability of data and materials

The data was accessible in NCBI with the direct link and login number: <https://www.ncbi.nlm.nih.gov/sra/?term=SRR8699030>, SRR8699030. <https://www.ncbi.nlm.nih.gov/sra/?term=SRR8699031>. <https://www.ncbi.nlm.nih.gov/sra/?term=SRR8699032>, SRR8699032. <https://www.ncbi.nlm.nih.gov/sra/?term=SRR8699033>, SRR8699033.

Declarations

Ethics approval and consent to participate

Not applicable.

Consent for publication

Not applicable.

Competing interests

The authors declare that they have no conflicts of interest.

Author details

¹School of Pharmacy, Nanjing University of Chinese Medicine, Nanjing 210000, China. ²College of Hanlin, Nanjing University of Chinese Medicine, Taizhou 225300, China. ³Jiangsu Collaborative Innovation Center of Chinese Medicinal Resources Industrialization, Nanjing University of Chinese Medicine, Nanjing 210000, China.

Received: 6 January 2021 Accepted: 4 May 2021

Published online: 25 June 2021

References

- Zhou JY, et al. Volatiles released by endophytic *Pseudomonas fluorescens* promoting the growth and volatile oil accumulation in *Atractylodes lancea*. *Plant Physiol Biochem*. 2016;101:132–40.
- Yu M, et al. *Atractylodes lancea* volatile oils attenuated helicobacter pylori NCTC11637 growth and biofilm. *Microb Pathog*. 2019;135:103641.
- Liu R, et al. The Suppressive Effects of the Petroleum Ether Fraction from *Atractylodes lancea* (Thunb.) DC. On a Collagen-Induced Arthritis Model. *Phytother Res*. 2016;30(10):1672–9.
- Wei Y, et al. *Atractylodes lancea* rhizome water extract reduces triptolide-induced toxicity and enhances anti-inflammatory effects. *Chin J Nat Med*. 2017;15(12):905–11.
- Zhang WJ, et al. *Atractylodes lancea* Rhizoma: A review of its traditional uses, phytochemistry, pharmacology, toxicology and quality control. *J Ethnopharmacol*. 2020;266:113415.
- Mathema VB, Chaijaroenkul W, Na-Bangchang K. Cytotoxic activity and molecular targets of atracylodin in cholangiocarcinoma cells. *J Pharm Pharmacol*. 2019;71(2):185–95.
- Na-Bangchang K, Plengsuriyakarn T, Karbwang J. Research and Development of *Atractylodes lancea* (Thunb.) DC. as a Promising Candidate for Cholangiocarcinoma Chemotherapeutics. *Evid Based Complement Alternat Med*. 2017;2017: 5929234.

8. Zhao M, et al. Selective fraction of *Atractylodes lancea* (Thunb.) DC. and its growth inhibitory effect on human gastric cancer cells. *Cytotechnology*. 2014;66(2):201–8.
9. Bai Y, et al. Atractylodin Induces Myosin Light Chain Phosphorylation and Promotes Gastric Emptying through Ghrelin Receptor. *Evid Based Complement Alternat Med*. 2017;2017:2186798.
10. Yang LP, et al. Network pharmacology study of ephedrae herba-atractylodis rhizoma in the treatment of novel coronavirus pneumonia. *J Chinese Med Materials*. 2020;43(7):1784–90.
11. Ma LJ, et al. Prescription rules and mechanisms of herbal prevention prescriptions for COVID-19 by data mining and network pharmacology. *Modernization of Traditional Chinese Medicine and Materia Medica*. World Science and Technology. 2020;22(3):566–72.
12. Li MY, et al. Effects of high temperature stress on chlorophyll fluorescence characteristics of *Atractylodes lancea* from different habitats. *Plant Physiology Journal*. 2015;51(11):1861–6.
13. D'Odorico P, et al. The global value of water in agriculture. *Proc Natl Acad Sci U S A*. 2020;117(36):21985–93.
14. Habermann E, et al. How does leaf physiological acclimation impact forage production and quality of a warmed managed pasture of *Stylosanthes capitata* under different conditions of soil water availability? *Sci Total Environ*. 2021;759:143505.
15. He J, Chua EL, Qin L. Drought does not induce crassulacean acid metabolism (CAM) but regulates photosynthesis and enhances nutritional quality of *Mesembryanthemum crystallinum*. *PLoS ONE*. 2020;15(3):e0229897.
16. Tan XL, et al. Melatonin delays leaf senescence of Chinese flowering cabbage by suppressing ABFs-mediated abscisic acid biosynthesis and chlorophyll degradation. *J Pineal Res*. 2019;67(1):e12570.
17. Rios CO, Siqueira-Silva AI, Pereira EG. How does drought affect native grasses' photosynthesis on the revegetation of iron ore tailings? *Environ Sci Pollut Res Int*. 2021;28:14797.
18. Iverma KK, et al. Characteristics of leaf stomata and their relationship with photosynthesis in *Saccharum officinarum* under drought and silicon application. *ACS Omega*. 2020;5(37):24145–53.
19. Pilon C, et al. Assessing stomatal and non-stomatal limitations to carbon assimilation under progressive drought in peanut (*Arachis hypogaea* L.). *J Plant Physiol*. 2018;231:124–34.
20. Zhao D, et al. A *Paeonia ostii* caffeoyl-CoA O-methyltransferase confers drought stress tolerance by promoting lignin synthesis and ROS scavenging. *Plant Sci*. 2021;303:110765.
21. Rangani J, et al. Regulation of ROS through proficient modulations of antioxidative defense system maintains the structural and functional integrity of photosynthetic apparatus and confers drought tolerance in the facultative halophyte *Salvadora persica* L. *J Photochem Photobiol B*. 2018;189:214–33.
22. Chugh V, et al. Differential antioxidative response of tolerant and sensitive maize (*Zea mays* L.) genotypes to drought stress at reproductive stage. *Indian J Biochem Biophys*. 2013;50(2):150–8.
23. Zhou J, et al. Study of effect of drought stress on physiological adaptation of seedlings of *Atractylodes lancea*. *China J Chin Materia Med*. 2008;33(19):2163–6.
24. Yang T, Ma S, Dai CC. Drought degree constrains the beneficial effects of a fungal endophyte on *Atractylodes lancea*. *J Appl Microbiol*. 2014;117(5):1435–49.
25. Liu Q, et al. Differentiation of essential oils in *Atractylodes lancea* and *Atractylodes koreana* by gas chromatography with mass spectrometry. *J Sep Sci*. 2016;39(24):4773–80.
26. Xu K, et al. Six new compounds from *Atractylodes lancea* and their hepatoprotective activities. *Bioorg Med Chem Lett*. 2016;26(21):5187–92.
27. Yang L, et al. Natural potent NAAA inhibitor atractylodin counteracts LPS-induced microglial activation. *Front Pharmacol*. 2020;11:577319.
28. Wang Y, et al. Comparison of the effects of fungal endophyte *Gilmaniella* sp. and its elicitor on *Atractylodes lancea* plantlets. *World J Microbiol Biotechnol*. 2012;28(2):575–84.
29. Sun P, et al. Functional diversification in the Nudix hydrolase gene family drives sesquiterpene biosynthesis in *Rosa wichurana*. *Plant J*. 2020;104(1):185–99.
30. Dwivedi V, et al. Functional characterization of a defense-responsive bulbosol/elemol synthase from potato. *Physiol Plant*. 2021;171(1):7–21.
31. Abdollahi Mandoulakani B, Eyvazpour E, Ghadimzadeh M. The effect of drought stress on the expression of key genes involved in the biosynthesis of phenylpropanoids and essential oil components in basil (*Ocimum basilicum* L.). *Phytochemistry*. 2017;139:1–7.
32. Huang Q, et al. Differential Gene Expression between Leaf and Rhizome in *Atractylodes lancea*: A Comparative Transcriptome Analysis. *Front Plant Sci*. 2016;7:348.
33. Ahmed S, et al. The Transcript Profile of a Traditional Chinese Medicine, *Atractylodes lancea*, Revealing Its Sesquiterpenoid Biosynthesis of the Major Active Components. *PLoS ONE*. 2016;11(3):e0151975.
34. Huang L, et al. Top-geoherbs of traditional Chinese medicine: common traits, quality characteristics and formation. *Front Med*. 2011;5(2):185–94.
35. Li Y, et al. The effect of developmental and environmental factors on secondary metabolites in medicinal plants. *Plant Physiol Biochem*. 2020;148:80–9.
36. Omid H, et al. Balangu (*Lallemantia* sp.) growth and physiology under field drought conditions affecting plant medicinal content. *Plant Physiol Biochem*. 2018;130:641–6.
37. Ashrafi M, et al. Effect of drought stress on metabolite adjustments in drought tolerant and sensitive thyme. *Plant Physiol Biochem*. 2018;132:391–9.
38. Kruse J, et al. Optimization of photosynthesis and stomatal conductance in the date palm *Phoenix dactylifera* during acclimation to heat and drought. *New Phytol*. 2019;223(4):1973–88.
39. Hu L, Wang Z, Huang B. Diffusion limitations and metabolic factors associated with inhibition and recovery of photosynthesis from drought stress in a C perennial grass species. *Physiol Plant*. 2010;139(1):93–106.
40. Carmo-Silva E, et al. Phenotyping of field-grown wheat in the UK highlights contribution of light response of photosynthesis and flag leaf longevity to grain yield. *J Exp Bot*. 2017;68(13):3473–86.
41. Chastain DR, et al. Water deficit in field-grown *Gossypium hirsutum* primarily limits net photosynthesis by decreasing stomatal conductance, increasing photorespiration, and increasing the ratio of dark respiration to gross photosynthesis. *J Plant Physiol*. 2014;171(17):1576–85.
42. Marček T, et al. Metabolic response to drought in six winter wheat genotypes. *PLoS ONE*. 2019;14(2):e0212411.
43. Singh SK, et al. Carbon dioxide diffusion across stomata and mesophyll and photo-biochemical processes as affected by growth CO₂ and phosphorus nutrition in cotton. *J Plant Physiol*. 2013;170(9):801–13.
44. Huang F, et al. Rubisco accumulation factor 1 (Raf1) plays essential roles in mediating Rubisco assembly and carboxysome biogenesis. *Proc Natl Acad Sci U S A*. 2020;117(29):17418–28.
45. Sun J, et al. Decrease in leaf sucrose synthesis leads to increased leaf starch turnover and decreased RuBP regeneration-limited photosynthesis but not Rubisco-limited photosynthesis in Arabidopsis null mutants of SPSA1. *Plant Cell Environ*. 2011;34(4):592–604.
46. De Porcellinis AJ, et al. Overexpression of bifunctional fructose-1,6-bisphosphatase/sedoheptulose-1,7-bisphosphatase leads to enhanced photosynthesis and global reprogramming of carbon metabolism in *Synechococcus* sp. *PCC 7002*. *Metab Eng*. 2018;47:170–183.
47. Dorion S, et al. A large decrease of cytosolic triosephosphate isomerase in transgenic potato roots affects the distribution of carbon in primary metabolism. *Planta*. 2012;236(4):1177–90.
48. Sharma DK, et al. QTLs and Potential Candidate Genes for Heat Stress Tolerance Identified from the Mapping Populations Specifically Segregating for Fv/Fm in Wheat. *Front Plant Sci*. 2017;8:1668.
49. Makonya GM, et al. Chlorophyll fluorescence and carbohydrate concentration as field selection traits for heat tolerant chickpea genotypes. *Plant Physiol Biochem*. 2019;141:172–82.
50. Lv Y, et al. Photochemistry and proteomics of ginger (*Zingiber officinale* Roscoe) under drought and shading. *Plant Physiol Biochem*. 2020;151:188–96.
51. Nawae W, et al. Differential expression between drought-tolerant and drought-sensitive sugarcane under mild and moderate water stress as revealed by a comparative analysis of leaf transcriptome. *PeerJ*. 2020;8:e9608.
52. Su L, et al. A novel system for evaluating drought-cold tolerance of grapevines using chlorophyll fluorescence. *BMC Plant Biol*. 2015;15:82.
53. Hamdani S, et al. Changes in the photosynthesis properties and photo-protection capacity in rice (*Oryza sativa*) grown under red, blue, or white light. *Photosynth Res*. 2019;139(1–3):107–21.

54. Jha RK, et al. Introgression of a novel cold and drought regulatory-protein encoding CORA -like gene, SbCCR, induced osmotic tolerance in transgenic tobacco. *Physiol Plant*. 2021;172:1170–88.
55. Singh DP, et al. Microbial inoculation in rice regulates antioxidative reactions and defense related genes to mitigate drought stress. *Sci Rep*. 2020;10(1):4818.
56. Zhang, C., et al., Drought tolerance in alfalfa (*Medicago sativa L.*) varieties is associated with enhanced antioxidative protection and declined lipid peroxidation. *J Plant Physiol*, 2019. 232: p. 226–240.
57. Rezaian M, Niknam V, Ebrahimzadeh H. Penconazole and calcium ameliorate drought stress in canola by upregulating the antioxidative enzymes. *Funct Plant Biol*. 2020;47(9):825–39.
58. Adebayo AR, Sebetha ET. Data on influence of different nitrogen fertilizer rates and plant density on grain yield and yield components of Water Efficient Maize (WEMA) variety. *Data Brief*. 2020;30:105582.
59. Paradiso A, et al. ROS Production and Scavenging under Anoxia and Re-Oxygenation in Arabidopsis Cells: A Balance between Redox Signaling and Impairment. *Front Plant Sci*. 2016;7:1803.
60. Barros Junior U.d.O., et al. Unraveling the roles of brassinosteroids in alleviating drought stress in young Eucalyptus urphylla plants: Implications on redox homeostasis and photosynthetic apparatus. *Physiol Plant*. 2021;172:748–661.
61. Esteban R, et al. On the recalcitrant use of Arnon's method for chlorophyll determination. *New Phytol*. 2018;217:474–6.
62. Hao A, et al. Effects of substrate and water depth of a eutrophic pond on the physiological status of a submerged plant *Vallisneria natans*. *PeerJ*. 2020;8:e10273.
63. Yang S, Zhang J, Chen L. Growth and physiological responses of *Pennisetum sp.* to cadmium stress under three different soils. *Environ Sci Pollut Res Int*. 2021;28:14867.
64. National Pharmacopoeia Committee. Pharmacopoeia of People's Republic of China. Part 4. Beijing: Chemical Industry Press; 2020. p. 233.

Publisher's Note

Springer Nature remains neutral with regard to jurisdictional claims in published maps and institutional affiliations.

Ready to submit your research? Choose BMC and benefit from:

- fast, convenient online submission
- thorough peer review by experienced researchers in your field
- rapid publication on acceptance
- support for research data, including large and complex data types
- gold Open Access which fosters wider collaboration and increased citations
- maximum visibility for your research: over 100M website views per year

At BMC, research is always in progress.

Learn more biomedcentral.com/submissions

